Journal of Engineering and Applied Sciences
MEDWELL PUBLICATIONS

Design and Implementation of Reconfigurable Microstrip Patch Antenna for Cognitive Radio Applications

Najim Abdallah Jazea
Department of Electrical Engineering, College of Engineering, Mustansiriyah University, Baghdad, Iraq

Key words: Reconfigurable, cognitive radio, MSPA, broadband antenna

Corresponding Author:
Najim Abdallah Jazea
Department of Electrical Engineering, College of Engineering, Mustansiriyah University, Baghdad, Iraq

Page No.: 3697-3707
Volume: 15, Issue 22, 2020
ISSN: 1816-949x
Journal of Engineering and Applied Sciences

Abstract: This study focuses on the design and analysis of a reconfigurable antenna that can be integrated into the CR systems. A dual-port "interweave" CR antenna system in which an antenna structure is proposed and designed. This design is composed of an elliptical disk radiator sensing antenna that covers a frequency range of (1.8-11) GHz and a dual-band reconfigurable communicating antenna in the form of a modified dual-band rectangular radiator. By controlling the length of a stub attached to the communicating antenna with the aid of two PIN diodes, the dual-band antenna can reconfigure its resonant frequencies to (2, 2.2 GHz), (3.25, 3.8 GHz) and (4.3, 5.6 GHz).

INTRODUCTION

Multi antennas were needed to cover the different frequency bands of the different standards such as Worldwide Interoperability for Microwave Access (WiMAX) and Wireless Local Area Network (WLAN)[1]. The reconfigurable antenna concept led to decrease the number of antennas existing in a certain device[2]. Reconfiguring an antenna is obtained through the change of its major characteristics such as frequency, polarization or radiation. Reconfigurable antennas can handle complex system requirements by variation their geometrical structure and electrical behavior[3]. The reconfigurable antenna can also be built in more complex systems as Multiple-Input Multiple-Output (MIMO) and/or Cognitive Radio (CR) systems[4, 5]. Cognitive Radio (CR) systems require antenna systems that have the capability to change identification in a communication environment and be able to respond appropriately[6]. The CR concept was first presented formally in an article by Mitola in 1999 by increasing the flexibility of personal wireless services during a new language called the Radio Knowledge Representation Language (RKRL)[7]. PIN diode switches are used to alter the effective length of the antenna to communicate at the most important frequencies in the range of the sensed spectrum[8]. The interweave CR system is continuously monitoring the unutilized channels (white spaces) in a certain frequency spectrum owned by other wireless systems[9]. Efficient spectrum usage and maximize the CR channel throughput is achieved by minimizing the interference with other wireless systems[10]. The interweave CR system has two types of antennas, the first antenna is used to sense the UWB frequency spectrum and continuously monitor the primary and secondary user's activity on the CR environment which known as sensing antenna[11]. The second antenna known as communicating antenna which uses those unutilized frequencies and achieves the data transfer[12]. The communicating antenna is a reconfigurable antenna that is accomplished on the CR platform for the efficient usage of the frequency spectrum by adjusting its fundamental operating parameters to adapt the frequency-band holes[13, 14]. There are some Challenges of Interweave CR Antennas[15]. The first challenge is to

minimize the overall area that contains both antennas without increasing the mutual coupling between the two antennas or degrade antenna gain, quality factor and bandwidth[16]. The second challenge is the appropriate coupling level between the two antennas using isolation technique, to minimize the crosstalk effect between the sensing and reconfigurable antennas[17]. The acceptable coupling level between the two-port antennas to be any value that is <-15 dB[18, 19].

The third challenge is the production of omnidirectional radiation pattern of the sensing antenna, where the major purpose of a CR device is to discover the idle bands instantly at any particular location via. its sensing antenna[20]. This is generally achieved by producing an equal radiation pattern in all directions.

MATERIALS AND METHODS

Dual-band reconfigurable slotted patch communicating antenna design: The proposed antenna is a compact rectangular microstrip patch at a resonant frequency of 3.5 GHz using the inset feed technique. The antenna is fabricated on an FR4 substrate with dielectric permittivity ε_r = 4.3, height h = 1.6 mm and loss tangent tanδ = 0.025. The radiating patch dimensions are calculated as (W_p = 26.3 mm and L_p = 20.2 mm) according the basic equations by Chen and Prasad[21]. The parametric study is carried out on the modification structure to obtain the target performance with better and smaller dimensions. Since, the size is an important constraint for the antenna to be compatible with interweave CR, therefore, some modification steps will be achieved for size minimization. A staircase defective partial ground structure as shown in Fig. 1a is used to improve the bandwidth by decreasing the capacitance between the ground plane and the patch[22]. This configuration exhibits single resonance mode at 3.8 GHz as displayed in Fig. 2 (ANT 1). Then, a circular slot with Radius (Rs) is created with the radiating patch leads to size reduction, since, the effective wavelength is increased[23] (as shown in Fig. 1b). A dual-band is obtained at frequencies 3.6 and 7.3 GHz, respectively as depicted in Fig. 2 (ANT 2). By etching inverted L-shaped strip at one edge of the patch with dimensions ($1\times L_{strip}$) mm^2, the second resonance frequency is at 5.7 GHz as shown in Fig. 2 (ANT 3). Figure 1d showed the final modification by rounding the lower edges of the patch and adjusting the strip length to the improvement of the impedance matching. Resonances at 3.3GHz and 5.5GHz are achieved as shown in Fig. 2 (Proposed ANT). This is useful for WiMAX and WLAN applications.

To get reconfigurable properties for this antenna, two PIN diodes are embedded into the L-shaped strip line. The RF switches are located at carefully chosen locations and they operate to change the effective length of the strip that results in tuning the resonant frequencies of the communicating antenna. The final structure of the proposed reconfigurable antenna is shown in Fig. 3 and the antenna design specifications are listed in details in Table 1.

Elliptical disc monopole UWB sensing antenna: An elliptical disk antenna is utilized as a UWB sensing antenna as shown in Fig. 4. The elliptical patch has a major axis radius (a) and minor axis radius (b). The radiating patch is fed by 50 Ω microstripline along its major axis. The elliptical radiating patch is a modified version of the circular patch antenna in which an improved frequency bandwidth is achieved due to an increase in the ellipticity ratio[23]. To calculate the antenna lower resonant frequency corresponding to impedance bandwidth S11 = -10 dB, the following equation is used[24, 25]:

Table 1: The best dimensions of the proposed antenna (Unit: mm)

W_1	W_2	W_3	W_4	W_5	W_6	W_f	L_1
12.25	14	2.23	6	6	6.15	3	8.75
L_2	L_3	L_4	L_5	L_6	L_f	Lstrip	r_s
4	4.6	2	2	4.4	9	17.3	5

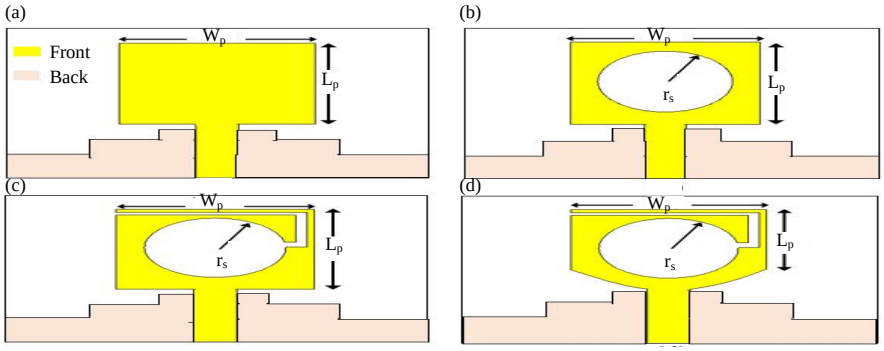

Fig. 1(a-d): Design evolution of the proposed antenna of the reconfigurable antenna, (a) ANT 1, (b) ANT 2, (c) ANT 3 and (d) Proposed ANT

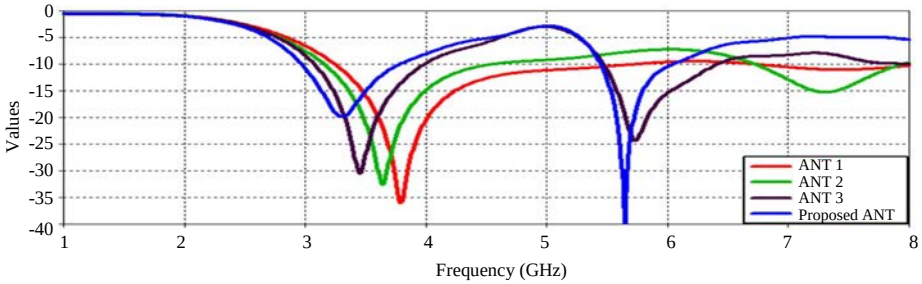

Fig. 2: Impedance bandwidth of antenna design steps

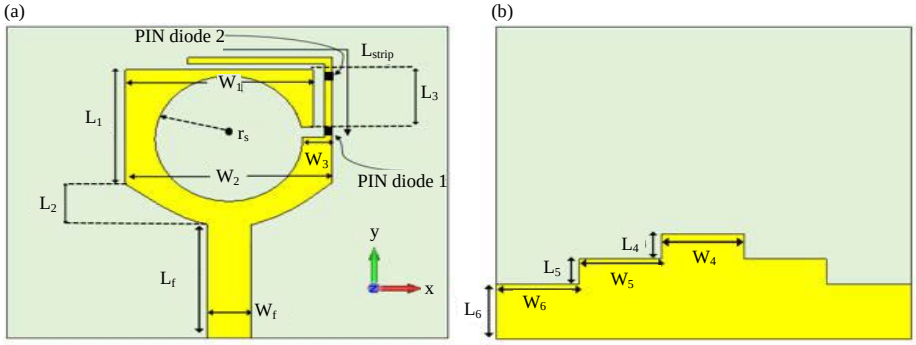

Fig. 3(a, b): The structure of the proposed reconfigurable antenna for interweave cognitive radio system, (a) Front view and (b) Back view

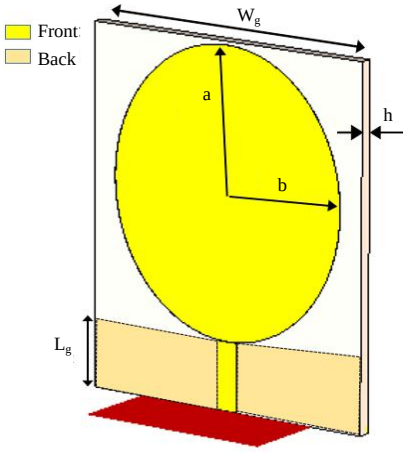

Fig. 4: A prototype elliptical patch antenna

$$f_{low}[GHz] = \frac{7.2}{2a + \frac{b}{4} + g_0} \quad (1)$$

Where:

a = Patch major axis (cm),
b = Patch minor axis (cm)
g_0 = Displacement between the elliptical patch and the ground (cm) = 0.5 mm

Equal values for each of (a) and (b) parameters are set initially into Eq. 1 as 18 mm with a target of wideband

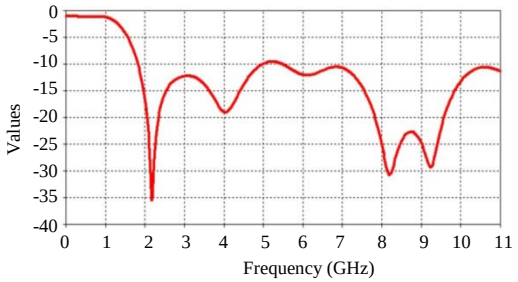

Fig. 5: The reflection coefficient of the prototype

characteristics. The impedance bandwidth of the prototype elliptical patch is shown in Fig. 5. It is clear that, the matching is poor and thus it is required to make some modifications in the effective parameters. In this design, the modifications will be done on ground plane later in the performance of the elliptical patch antenna is compared to the circular patch antenna for different ellipticity ratios. Therefore, various combinations of major and minor axes are studied in Fig. 6. In this study, the patch area is maintained by increasing the major axis of the antenna and decreasing the minor axis of the elliptical patch. The simulated reflection coefficient is shifted to the lower frequency region by increasing the elliptical ratio.

Ground plane effect: A parametric study is carried out using CST Microwave studio to demonstrate the

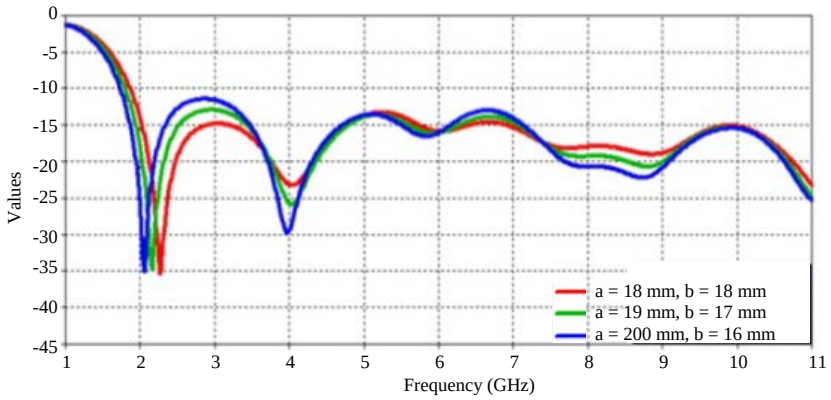

Fig. 6: The Simulated reflection coefficient for elliptical patch antenna various values of elliptical ratio

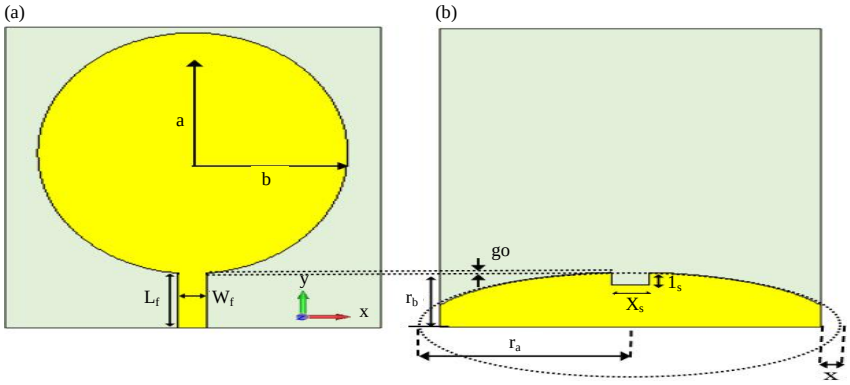

Fig. 7(a, b): The proposed design of UWB sensing antenna, (a) Front view and (b) Back view

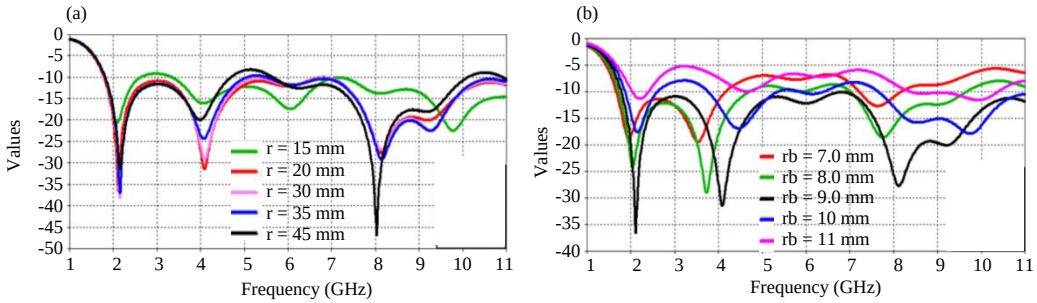

Fig. 8(a, b): The Simulated reflection coefficient for, (a) various values of (r_a) with (r_b) = 9 mm and (b) Various values of (r_b) with (r_a) =22 mm

effect of ground plane. The ground plane is chosen as semi-elliptical shape with a width and length of (r_a) and (r_b), respectively as shown in Fig. 7.

Figure 8 illustrates the simulated reflection coefficient characteristics study of different values of (r_a) and (r_b) when the other antenna parameters are a = 20 mm, b = 16 mm, g_0 = 0.5 mm. It is clear from Fig. 8a the adjustment in the ground plane width (r_a) with fixed (r_b) can slightly shift the lower resonance frequency and influence the impedance matching. As the width (r_a) increased, the impedance matching will be improved for both the upper and lower bands. The best value is found as 22 mm. Figure 8b shows the effect of ground plane length (r_b) on the impedance bandwidth with (r_a) fixed. As the length of the ground (r_b) increases from 7-11 mm, the resonance frequencies are shifted up to cover the wideband range (2.9-11) GHz. Hence, this distance is one of the parameters which affect the impedance matching. The best value is found as 9 mm.

The effect of ground plane offset width is also studied by the parameter (x) as shown in Fig. 9. It is clear that a minor effect occurs in the impedance matching of

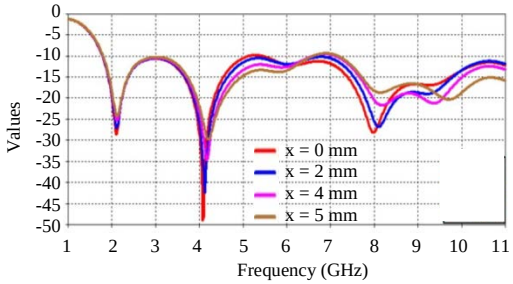

Fig. 9: The Simulated reflection coefficient for various

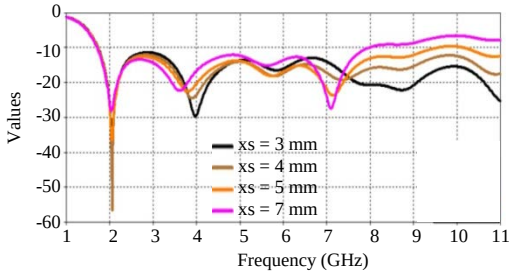

Fig. 10: The Simulated reflection coefficient values of x with (r_a) =22 mm and (r_b) =9 mm for various values of (x_s)

Table 2: The best dimensions of the UWB sensing antenna design (Unit: mm)

W_f	L_f	a	b	r_a	r_b	g_0	x	x_s	l_s
3	9.5	20	16	22	9	0.5	2	3	2

the upper frequency as the parameter (x) was varied. The best selected value is 2 mm. Finally, a rectangular slit is loaded into the ground plane in order to broaden the response and enhance the impedance matching[22]. The slit width (x_s) is investigated as shown in Fig. 10. It can be seen that the increasing of (x_s) parameter degrades the impedance matching of the upper frequency band. No effect has been observed at the lower frequency band. Therefore, the reflection coefficient of the upper frequency can be adjusted by the slit width parameter (x_s) and the best value is found as (x_s) is 3 mm.

After applying the parametric study on the effective parameters of the antenna, the best values of each one have been selected. The required UWB frequency spectrum range (3.1-10.6) GHz which allocated by the FCC commission is covered by the proposed antenna. Hence, this antenna is considered a good candidate for sensing the UWB function of the interweave CR platform with the design dimensions as listed in Table 2.

The composite interweave cr structure: The integration of the reconfigurable and the UWB antennas into a single substrate will form the intended dual-port interweave CR front end with an overall area of (W×L = 70×50) mm^2. Figure 11 illustrates the front and the back views of the

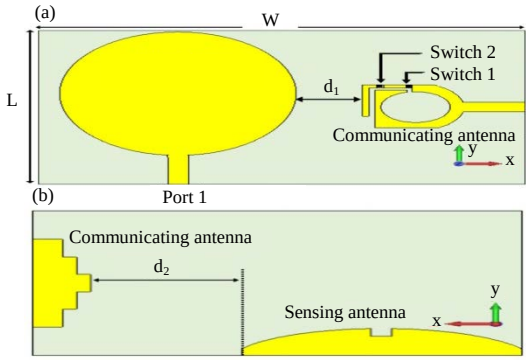

Fig. 11(a, b): Configuration of the proposed interweave cognitive radio, (a) Front view and (b) Back view

proposed antenna. The front view represents the patches of the communicating and the sensing antennas whereas the back view represents their ground planes. Dual ports have been used where the UWB sensing antenna is connected to port 1 while the reconfigurable communicating antenna is excited via. port 2. Since, the two antennas are printed on the same substrate, hence, the separation distance between them is taken into consideration. This distance has a direct effect in determining the mutual coupling. Therefore, it is essential to optimize the separation distance in the design of the interweave CR antennas. There is a trade-off between the separation and the mutual coupling between the sensing and the communicating antenna. In this design, the separation parameters (d1) and (d2) are found as (9.4) and (21.3) mm, respectively, to obtain mutual coupling <-15 dB over the whole operation frequency spectrum.

RESULTS AND DISCUSSION

The performances of the designed antenna configuration regarding reflection coefficients, mutual coupling, surface currents, radiation patterns and the gain for various switching states of the two PIN diodes have been studied and measured. The CST software package was used to produce the simulation while the measurements were achieved using AMITEC vector network analyzer VNA40. The obtained results have a small deviation from the simulated results due to many factors such as the imperfect fabrication process and the measurement environments as well as the imperfect soldering of the switches and the SMA connectors. Figure 12 shows the front and the back views of the prototype of the proposed antenna.

Reflection coefficient and mutual coupling

UWB sensing antenna: The reflection coefficient at the port (1) is shown in Fig. 13 which represents the

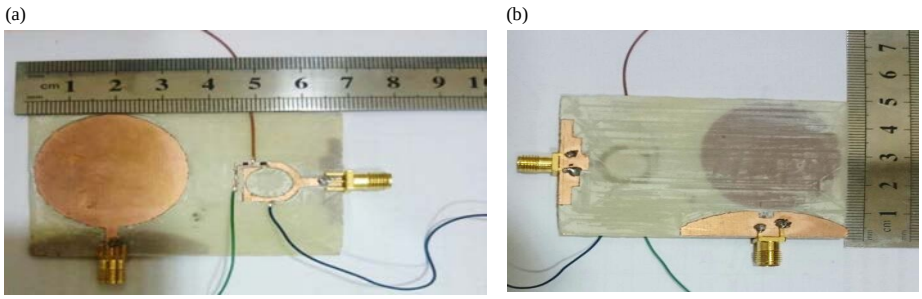

Fig. 12(a, b): Prototype of the fabricated interweave cognitive radio structure, (a) Front view and (b) Back view

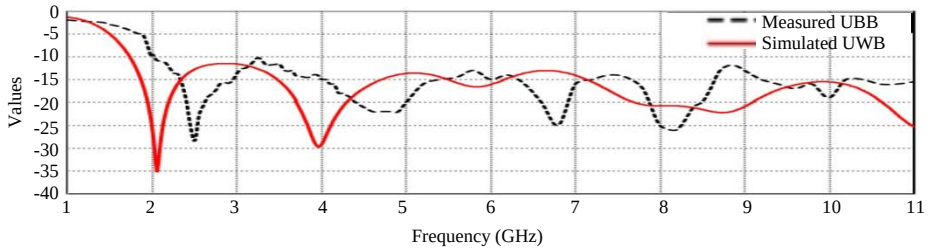

Fig. 13: The simulated and measured reflection coefficient at port of UWB sensing antenna

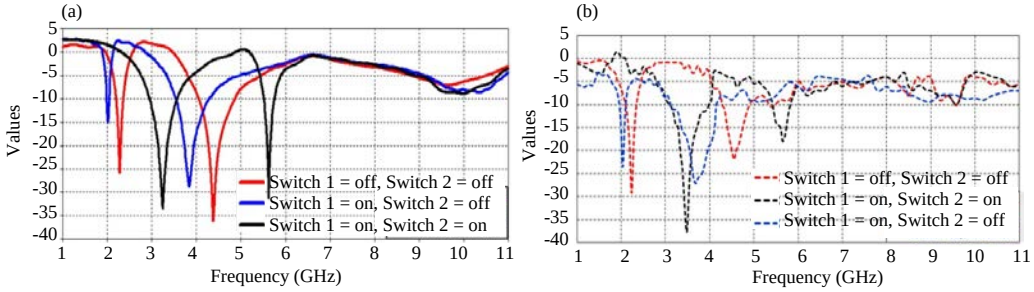

Fig. 14(a, b): The reflection coefficient at port (2) for various switching states of the reconfigurable antenna, (a) Simulated and (b) Measured

reflection coefficient of the sensing antenna. The reflection coefficient remains as it is for various switch states of the reconfigurable antenna. It is clear that, the antenna covers the entire frequency band specified for UWB applications.

Reconfigurable communicating antenna: The measured and simulated reflection coefficients at the port (2) for various switching states are illustrated in Fig. 14. The two PIN diodes will provide three evident resonance modes that lead to tuning the reconfigurable antenna within the range (2-6) GHz. The achieved resonance frequency bands of various switching states and the corresponding impedance bandwidth values (S22 parameter <-10 dB) are scheduled in Table 3.

Mutual coupling: As mentioned earlier, the essential issue in the design of dual-port CR antennas is in providing appropriate isolation between the ports. Figure 15 shows the mutual couplings between the two-ports over the entire sensing frequency spectrum. The mutual coupling between the two-ports is <-15 dB for the entire sensing band for various states of the PIN diodes.

Table 3: The resonance frequency bands of various switching states

Diode 1	Diode 2	Simulated	Measured (GHz)
ON	OFF	2-3.8	2.1-3.68
OFF	OFF	2.2-0.3	2.23-4.55
ON	ON	3.255.6	3.48-5.7

Current distribution: Figure 16 shows the simulated surface current distributions on the two antenna elements for different switching states. When the proposed structure is excited via port (1), the maximum current intensity (red color) is stronger in the lower band

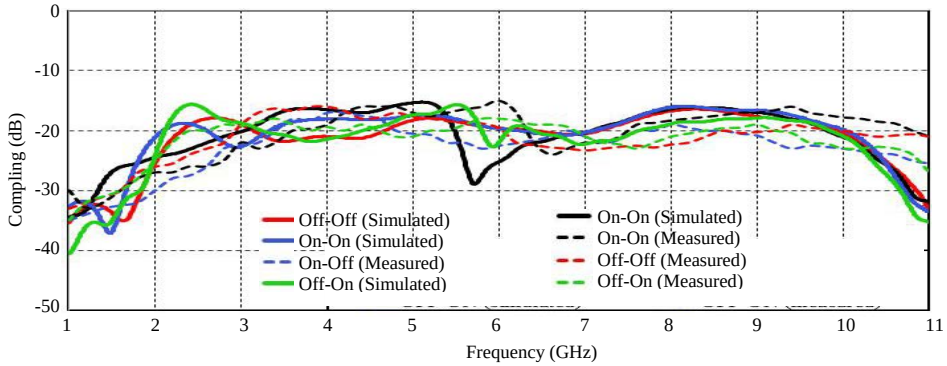

Fig. 15: The simulated (solid) and measured (dashed) mutual coupling for various switching states of interweave CR

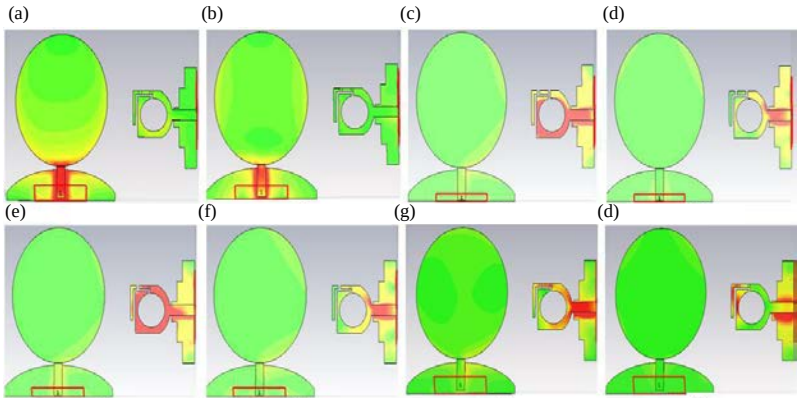

Fig. 16(a-h): The simulated surface currents, (a, b) Sensing antenna at 2 and 4 GHz, (c, d) Communicating antenna OFF-OFF at 2.2 and 4.3 GHz, (e, f) Communicating antenna ON-OFF at 2 and 3.8 GHz and (g, h) Communicating antenna ON-ON at 3.25 and 5.6 Ghz

compared to the upper band as shown in Fig. 16a, b. The high current density is concentrated at the feedline as well as the lower section of the elliptical patch which contributes to radiation. Meanwhile, the current excited at the port (2) approximately zero which ensures that both antennas are highly isolated.

In frequency reconfiguration mode (port 2) when all the switches are OFF sate, large surface current is concentrated around the left section of the patch while the parasitic strip is nearly isolated. Therefore, the antenna resonates at 2.2 and 4.3 GHz as displayed in Fig. 16c, d. In ON-OFF state, the maximum current intensity extends to the strip which is connected with patch via. switch 1. This makes the antenna to resonate at 2 and 3.8 GHz as shown in Fig. 16e, f. However, when both diodes are ON state, current flows at both the strip and the patch which makes the antenna to resonate at 3.25 and 5.6 GHz as shown in Fig. 16g, h.

Radiation pattern: The simulated and measured radiation patterns at different resonant frequencies of the two antennas are shown in Fig. 17.

The UWB antenna has nearly omnidirectional radiation patterns in the H-plane and bidirectional pattern in the E-plane. Figure 18-20 shows the effects of the switches on the measured and simulated patterns of the antenna in different states with different resonant frequencies over the operating bandwidth.

Antenna gain: The simulated and measured gains of the sensing and the communicating antenna elements are exhibited in Fig. 21-23.

The sensing antenna gain offers almost suitable gain over the whole UWB spectrum with a maximum value of 6.8 dBi. The communicating antenna gain for different switching states has an appropriate value for the various resonant frequencies with a maximum value of 5.5 dBi.

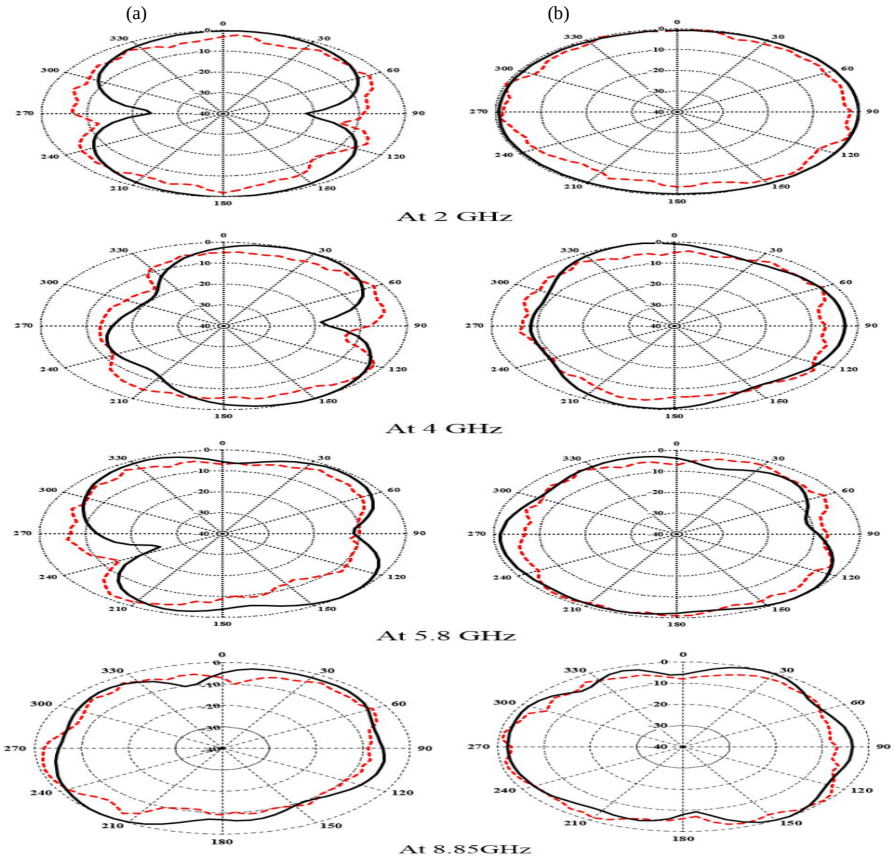

Fig. 17(a, b): The simulated (solid) and measured (dashed) radiation pattern of the UWB sensing antenna, (a) E-plane and (b) H-plane

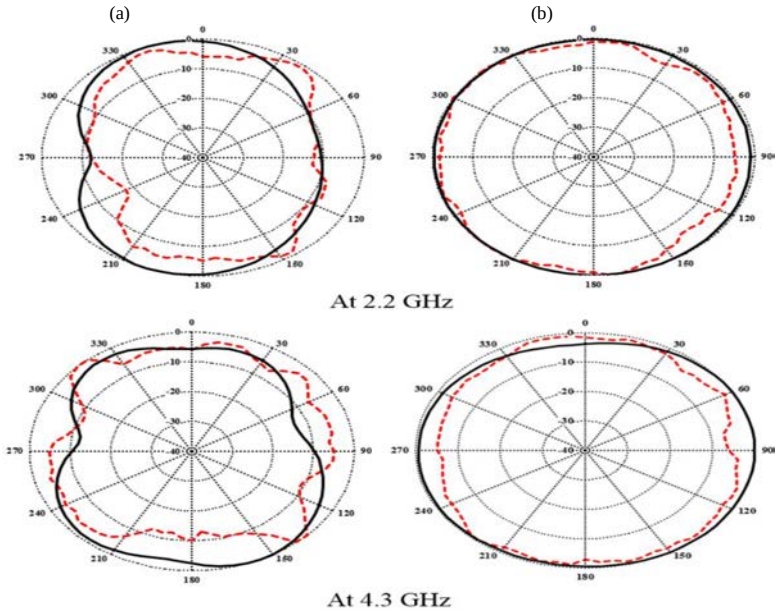

Fig. 18(a, b): The Simulated (solid) and measured (dashed) radiation patterns of the communicating antenna (all switches OFF), (a) E-plane and (b) H-plane

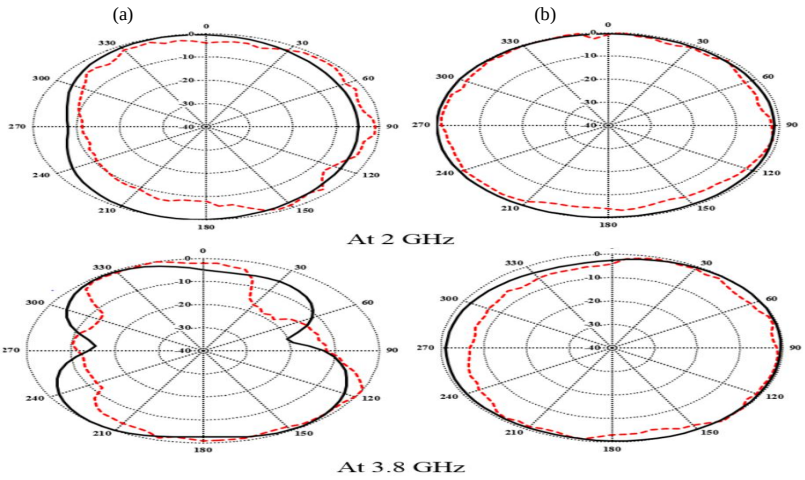

Fig. 19(a, b): The Simulated (solid) and measured (dashed) radiation patterns of the communicating antenna (Switch 1 = ON, Switch 2 = OFF), (a) E-plane and (b) H-plane

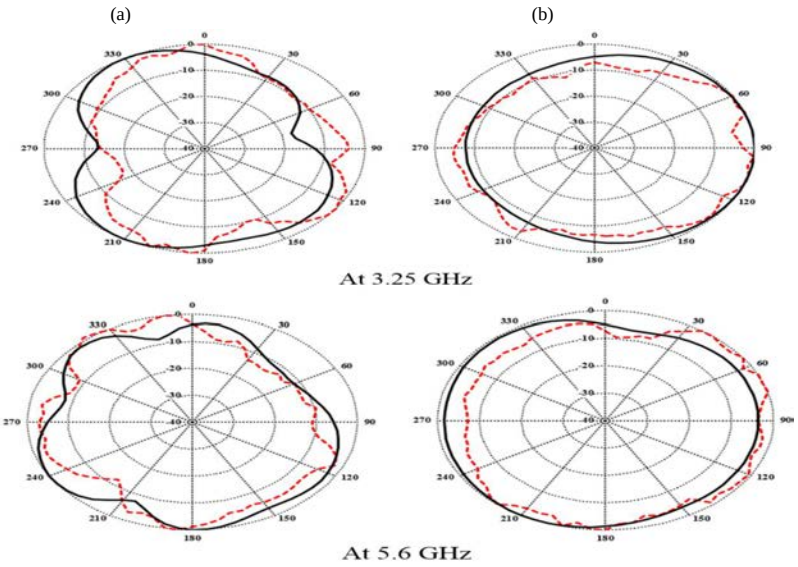

Fig. 20(a, b): The Simulated (solid) and measured (dashed) radiation patterns of the communicating antenna (all switches ON), (a) E-plane and (b) H-plane

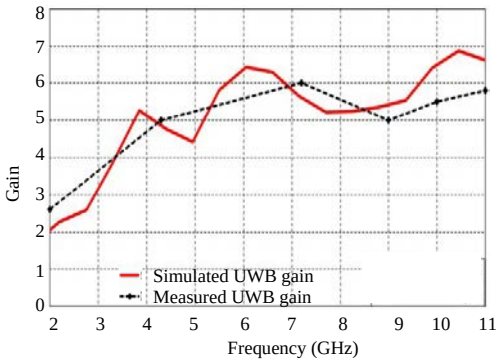

Fig. 21: The Simulated (solid) and measured

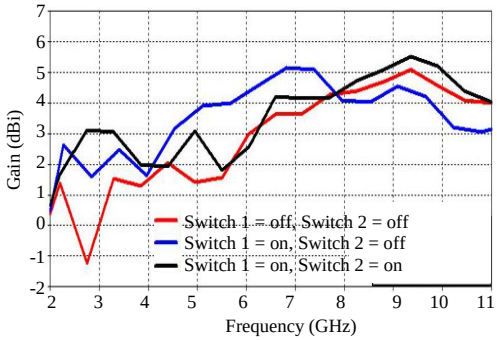

Fig. 22: The Simulated gain of different switching (dashed) gain of the UWB sensing antenna states for communicating antenna

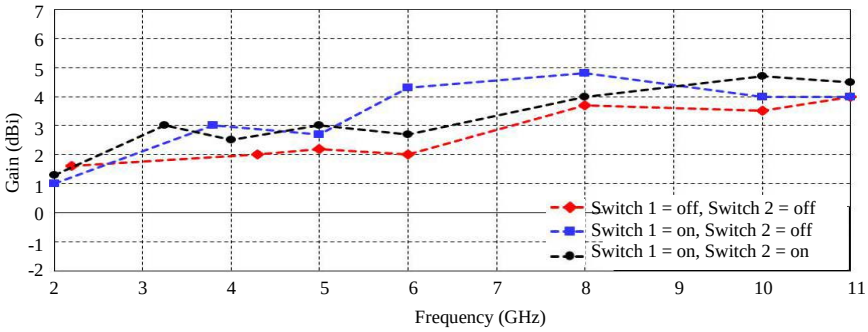

Fig. 23: The measured gain of different switching states for communicating antenna

CONCLUSION

The antenna system designed for cognitive radio is required to monitor the channel, search for white spaces (idle frequencies), identify the white spaces through software and communicate over these idle frequencies. Electrical reconfiguring techniques based on PIN diodes have been used in this antenna to realize the different design frequencies while maintaining a mostly simple geometry to the radiating structure. Design and analysis of a new dual-port interweave CR antenna has been presented in this work, of size of (70×50×1.6) mm^3 which can sense the spectrum from (1.8-11) GHz using an elliptical disc monopole antenna. Then, a dual-band reconfigurable slotted patch communicating antenna has been made to communicate in any of the 6 frequency states 2, 2.2, 3.25, 3.8, 4.3 and 5.6 GHz. Two PIN diode switches were used with simple D.C. biasing circuit integrated into the antenna. The mutual coupling between the two ports was found <-15 dB for the entire sensing band for various states of the PIN diodes.

REFERENCES

01. Biglieri, E., R. Calderbank, A. Constantinides, A. Goldsmith, A. Paulraj and H.V. Poor, 2007. MIMO Wireless Communications. Cambridge University Press, New York, USA.,.
02. Hugine, A.L., 2016. Antenna selection for a public safety cognitive radio. Ph.D. Thesis, Virginia Polytechnic Institute and State University, Blacksburg, Virginia.
03. Augustin, G., B.P. Chacko and T.A. Denidni, 2013. Dual Port Ultra Wideband Antennas for Cognitive Radio and Diversity Applications. In: Advancement in Microstrip Antennas with Recent Applications, Kishk, A. (Ed.). InTech, New, York, USA., pp: 203-226.
04. Pandharipande, V.M., 2013. Studies on reconfigurable printed antennas. Ph.D. Thesis, Osmania University, Hyderabad, India.
05. Costantine, J., Y. Tawk and C.G. Christodoulou, 2014. Reconfigurable Antennas and their Applications. In: Handbook of Antenna Technologies, Chen, Z.N. (Ed.). Springer, Singapore, pp: 1-30.
06. Tsoulos, G., 2006. MIMO System Technology for Wireless Communications. CRC Press, Boca Raton, London.
07. Fette, A.B., 2006. Cognitive Radio Technology. Newnes Publisher, New York, USA., Pages: 622.
08. Tawk, Y., J. Costantine and C.G. Christodoulou, 2013. Reconfigurable filtennas and MIMO in cognitive radio applications. IEEE. Trans. Antennas Propag., 62: 1074-1083.
09. Nella, A. and A.S. Gandhi, 2018. A survey on planar antenna designs for cognitive radio applications. Wireless Personal Commun., 98: 541-569.
10. Jassim, A.K. and R.H. Thaher, 2016. Calculate the optimum slot area of elliptical microstrip antenna for mobile application. Indonesian J. Electrical Eng. Comput. Sci., 16: 1364-1370.
11. Chen, R.H. and J.S. Row, 2008. Single-fed microstrip patch antenna with switchable polarization. IEEE. Trans. Antennas Propag., 56: 922-926.
12. Behdad, N. and K. Sarabandi, 2006. A varactor-tuned dual-band slot antenna. IEEE. Trans. Antennas Propag., 54: 401-408.
13. Tawk, Y., A.R. Albrecht, S. Hemmady, G. Balakrishnan and C.G. Christodoulou, 2010. Optically pumped frequency reconfigurable antenna design. IEEE. Antennas Wireless Propag. Lett., 9: 280-283.
14. Jassim, A.K. and H. Raad, 2019. Enhancement gain of broadband elliptical microstrip patch array antenna with mutual coupling for wireless communication. Indonesian J. Electr. Eng. Comput. Sci., 13: 401-408.
15. Rebeiz, G.M. and J.B. Muldavin, 2001. RF-MEMS switches and switch circuits. IEEE Microwave Mag., 2: 59-71.
16. Kramer, B.A., C.C. Chen and J.L. Volakis, 2008. Size reduction of a low-profile spiral antenna using inductive and dielectric loading. IEEE. Antennas Wirel. Propag. Lett., 7: 22-25.

17. Mazlouman, S.J., M. Soleiman, A. Mahanfar, C. Menon and R.G. Vaughan, 2011. Pattern reconfigurable square ring patch antenna actuated by a hemispherical dielectric elastomer. Electron. Lett., 47: 164-165.
18. Jassim, A.K. and R.H. Thaher, 2018. Design and analysis of broadband elliptical microstrip patch antenna for wireless communication. Telkomnika Telecommun. Comput. Electron. Control, 16: 2492-2499.
19. Hu, W., M.Y. Ismail, R. Cahill, J.A. Encinar and V.F. Fusco *et al*., 2007. Liquid crystal based reflectarray antenna with electronically switchable monopulse patterns. IEE Electron. Lett., 43. 10.1049/el:20071098
20. Costantine, J., Y. Tawk and C.G. Christodoulou, 2013. Design of reconfigurable antennas using graph models. Synth. Lectures Antennas, 5: 1-148.
21. Chen, K.C. and R. Prasad, 2009. Cognitive Radio Networks. Wiley, Hoboken, New Jersey, USA.,.
22. Zhao, Q. and A. Swami, 2007. A survey of dynamic spectrum access: Signal processing and networking perspectives. Proceedings of the IEEE International Conference on Acoustics, Speech and Signal Processing, Volume 4, April 15-20, 2007, Honolulu, HI., USA., pp: IV-1349-IV-1352.
23. Safarian, A. and P. Heydari, 2007. Silicon-Based RF Front-Ends for Ultra Wideband Radios. Springer, Netherlands,.
24. Hall, P.S., P. Gardner and A. Faraone, 2012. Antenna requirements for software defined and cognitive radios. Proc. IEEE., 100: 2262-2270.
25. Jassim, A.K. and R.H. Thaher, 2019. Design of MIMO (4x4) broadband antenna array for mm-wave wireless communication applications. Int. J. Eng. Appl. (IREA.), Vol. 7, No. 2. 10.15866/irea.v7i2. 16804